Обзор ArXiv:astro-ph, 18-23 апреля 2016 года

От Сильченко О.К.

Astro-ph: 1604.04632

On the properties of galaxies at the faint-end of the Hα luminosity function at $z \sim 0.62$ ⋆

Carlos Gómez-Guijarro[1,2], Jesús Gallego[1], Víctor Villar[1,3], Lucía Rodríguez-Muñoz[1,4], Benjamin Clément[5] and Jean-Gabriel Cuby[6]

[1] Departamento de Astrofísica y CC. de la Atmósfera, Facultad de CC. Físicas, Universidad Complutense de Madrid, Av. Complutense s/n, E-28040 Madrid, Spain
e-mail: cgguijarro@ucm.es
[2] Dark Cosmology Centre, Niels Bohr Institute, University of Copenhagen, Juliane Maries Vej 30, DK-2100 Copenhagen, Denmark
[3] European Space Astronomy Centre, PO Box 78, E-28691 Villanueva de la Cañada, Madrid, Spain
[4] Dipartimento di Fisica e Astronomia "G. Galilei", Universitá di Padova, Vicolo dell'Osservatorio 3, I-35122, Italy
[5] CRAL, Observatoire de Lyon, Université Lyon 1, 9 Avenue Ch. André, F-69561 Saint Genis Laval Cedex, France
[6] Aix Marseille Université, CNRS, LAM (Laboratoire d'Astrophysique de Marseille) UMR 7326, 13388, Marseille, France

Received 15 June 2015; accepted 14 April 2016

ABSTRACT

Context. Studies measuring the star formation rate density, luminosity function and properties of star-forming galaxies are numerous. However, it exists a gap at $0.5 < z < 0.8$ in Hα-based studies.
Aims. Our main goal is to study the properties of a sample of faint Hα emitters at $z \sim 0.62$. We focus on their contribution to the faint-end of the luminosity function and derived star formation rate density, characterising their morphologies and basic photometric and spectroscopic properties.

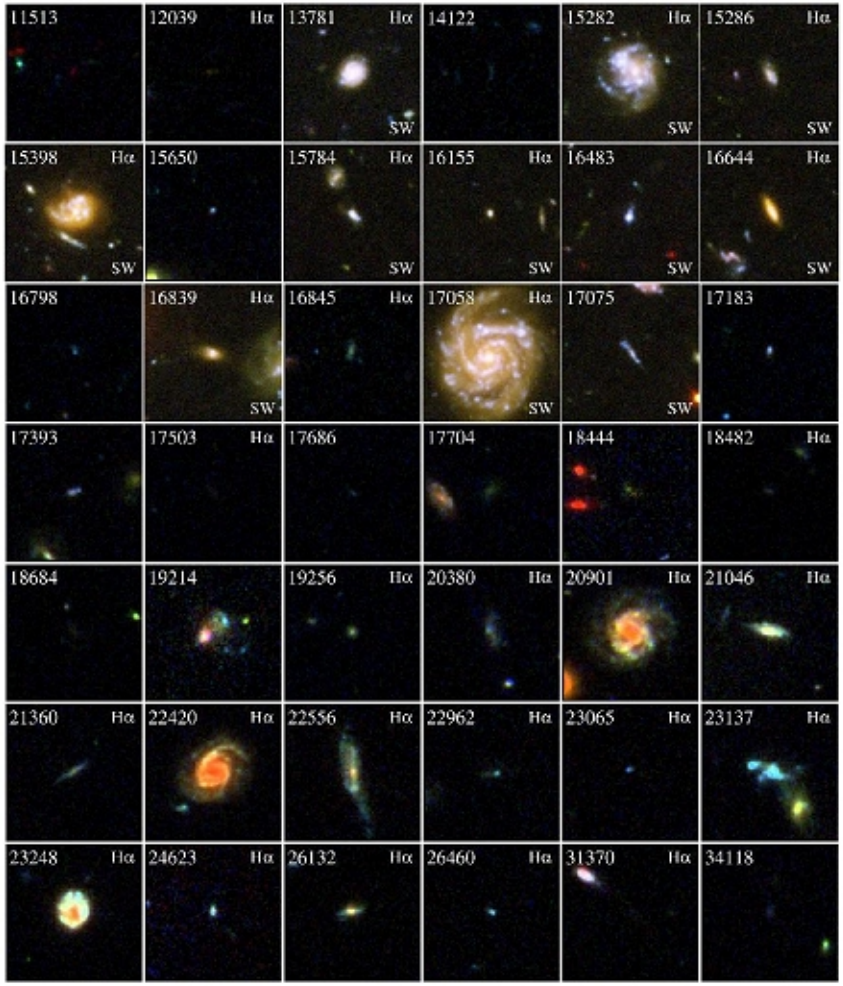

Fig. 3. RGB postage stamps of the 42 objects in our raw sample with CANDELS counterpart. North is up, East to the left and the images have a size of 5″×5″. The CANDELS ID is in the upper left corner. Those classified as Hα emitters show this label in the upper right corner. Those images built with UDF Skywalker show the label SW in the bottom right corner.

Table 2. Visual morphological classification. First row shows the numbers(percentages) over the 'Total' sample including the 42 objects with CANDELS counterpart. The second row includes just the numbers(percentages) over the objects classified as Hα emitters.

Sample	Spiral	Disk	Spheroid	Compact	Irregular	Unclassifiable
Total	6(14%)	15(36%)	4(9%)	2(5%)	13(31%)	2(5%)
Hα	6(21%)	13(46%)	3(11%)	1(4%)	3(11%)	2(7%)

Свойства галактик выборки

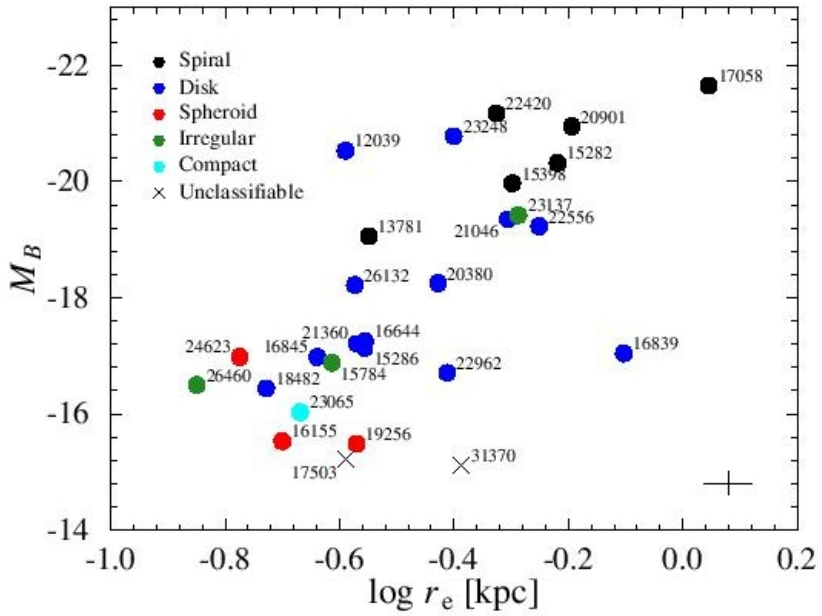

Fig. 4. Rest-frame *B* band absolute magnitude vs. effective radius measured in the F160W band for the 42 objects in our sample with CANDELS counterpart. We show the morphological classification of each object as it is indicated in the legend. Error bars are indicated in the bottom right corner.

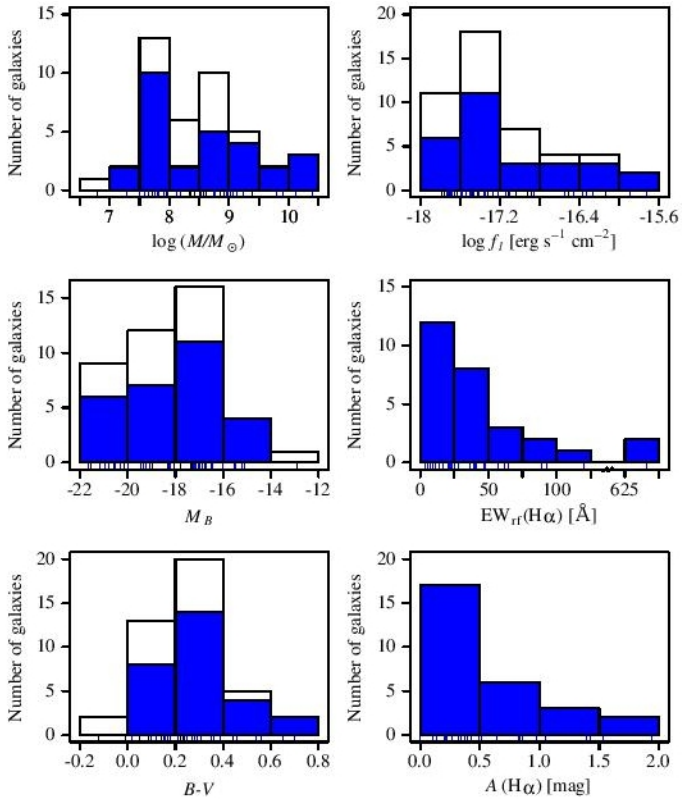

Результаты

Table 6. Average values and deviations of several physical properties for the 'Hα' sample. The Sérsic index values just consider the objects with structural parameters available in van der Wel et al. (2012).

Category	$\log(M/M_\odot)$	$\log r_e$ (kpc)	n	M_B	$EW_{rf}(H\alpha)$ (Å)	$A(H\alpha)$ (mag)	SFR_{cor} ($M_\odot$ yr^{-1})
Disk (72%)	8.94 ± 0.85	-0.40 ± 0.20	0.92 ± 0.31	-18.88 ± 1.69	61 ± 140	0.40 ± 0.34	0.52 ± 0.81
Compact (21%)	7.71 ± 0.22	-0.70 ± 0.10	1.87 ± 0.87	-16.24 ± 0.65	141 ± 250	0.97 ± 0.65	0.13 ± 0.07
Unclassifiable (7%)	7.54 ± 0.06	-0.49 ± 0.14	(...)	-15.16 ± 0.07	91 ± 40	1.24 ± 0.27	0.08 ± 0.01

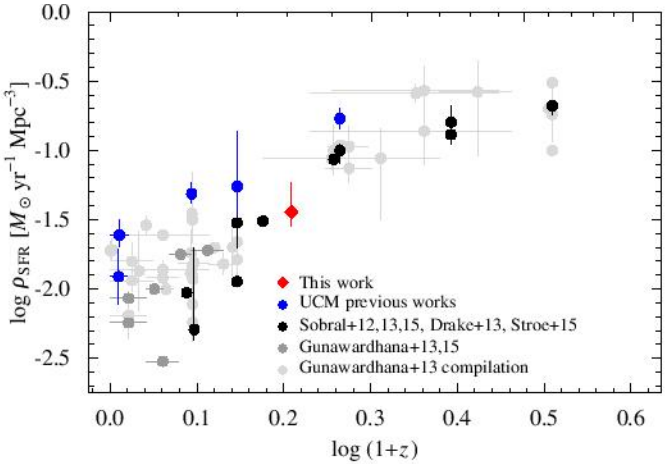

Fig. 14. Evolution of the SFRD with redshift from Hα studies. This work is shown in red filled diamond. We emphasise previous UCM works in blue filled circles. The black circles correspond to the last studies Sobral et al. (2012) at $z \sim 1.47$, Sobral et al. (2013) at $z \sim 0.4, 0.84, 1.47, 2.23$, Drake et al. (2013) at $z \sim 0.25, 0.4, 0.5$, Sobral et al. (2015) at $z \sim 0.8$ and Stroe & Sobral (2015) at $z \sim 0.2$. The compilation in Table B1 of Gunawardhana et al. (2013) is included in grey filled circles. The results in Table 2 of Gunawardhana et al. (2013) from both GAMA and SDSS-DR7 data are shown in dark grey filled circles, substituted by the more recent values in Gunawardhana et al. (2015) for the redshift bins $0.1 < z < 0.15$, $0.17 < z < 0.24$, and $0.24 < z < 0.35$.

Astro-ph: 1604.05193

Simulations of ram-pressure stripping in galaxy–cluster interactions

Dominik Steinhauser[1], Sabine Schindler[1], and Volker Springel[2, 3]

[1] Institut für Astro- und Teilchenphysik Universität Innsbruck, Technikerstrasse 25/8, 6020 Innsbruck, Austria
[2] Heidelberger Institut für Theoretische Studien, Schloss-Wolfsbrunnenweg 35, 69118 Heidelberg, Germany
[3] Zentrum für Astronomie der Universität Heidelberg, Astronomisches Recheninstitut, Mönchhofstr. 12-14, 69120 Heidelberg

April 19, 2016

ABSTRACT

Context. Observationally, the quenching of star-forming galaxies appears to depend both on their mass and environment. The exact cause of the environmental dependence is still poorly understood, yet semi-analytic models (SAMs) of galaxy formation need to parameterise it to reproduce observations of galaxy properties.
Aims. In this work, we use hydrodynamical simulations to investigate the quenching of disk galaxies through ram-pressure stripping (RPS) as they fall into galaxy clusters with the goal of characterising the importance of this effect for the reddening of disk galaxies.

Модели галактик

		G1a (G1b, G1c)	G2
c		9	10
v_{200}	$\left[\mathrm{km\,s^{-1}}\right]$	170	110
λ		0.033	0.04
m_d		0.041	0.041
m_b		0.01367	0
f_{gas}		0.35	0.35
z_0		0.2	0.2
M_{DM}	$\left[h^{-1}\,\mathrm{M}_\odot\right]$	1.02×10^{12}	2.95×10^{11}
$M_{\mathrm{gas,d}}$	$\left[h^{-1}\,\mathrm{M}_\odot\right]$	1.64×10^{10}	4.44×10^{9}
$M_{\star,\mathrm{d}}$	$\left[h^{-1}\,\mathrm{M}_\odot\right]$	3.04×10^{10}	8.25×10^{9}
$M_{\star,\mathrm{b}}$	$\left[h^{-1}\,\mathrm{M}_\odot\right]$	1.56×10^{10}	0
$M_{\mathrm{gas,h}}$	$\left[h^{-1}\,\mathrm{M}_\odot\right]$	$6.24(3.12, 0.0625) \times 10^{10}$	1.26×10^{9}
r_0	$\left[h^{-1}\,\mathrm{kpc}\right]$	2.60943	2.2063
a_b	$\left[h^{-1}\,\mathrm{kpc}\right]$	0.5219	-

Notes. We specify the principal structure of these models (in particular total mass and disk) with choices for the concentration parameter c, rotation velocity v_{200} at the virial radius r_{200}, and spin parameter λ. The values m_d and m_b are the disk and bulge mass fractions, respectively, with f_{gas} specifying the initial amount of gas in the disk and z_0 giving the disk height as a fraction of the disk scale length r_0 (equal for both the

Галактика влетает в скопление

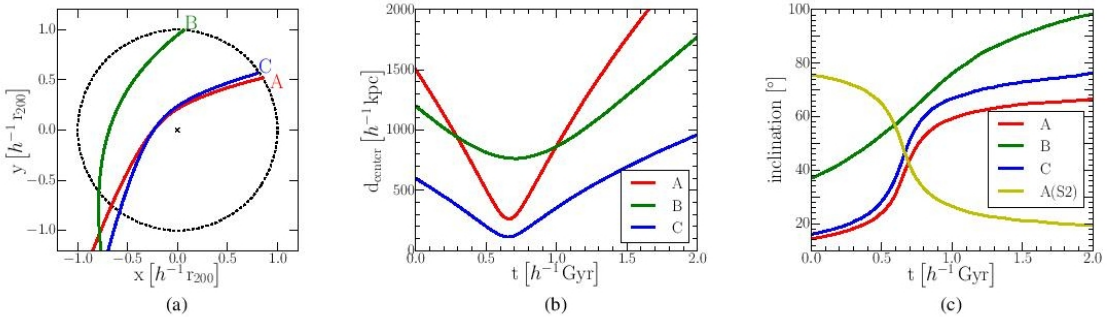

Fig. 2. Fiducial galaxy orbits adopted for studying the interaction of galaxy model G1a with the three different galaxy clusters constructed for the study. (a) Trajectories of the galaxy in clusters A, B, and C, scaled to the virial radius of the corresponding cluster. (b) Time evolution of the distance of the galaxy to the corresponding cluster centre. (c) Effective inclination angle of the galaxy (angle between the spin vector of the disk and its instantaneous velocity vector).

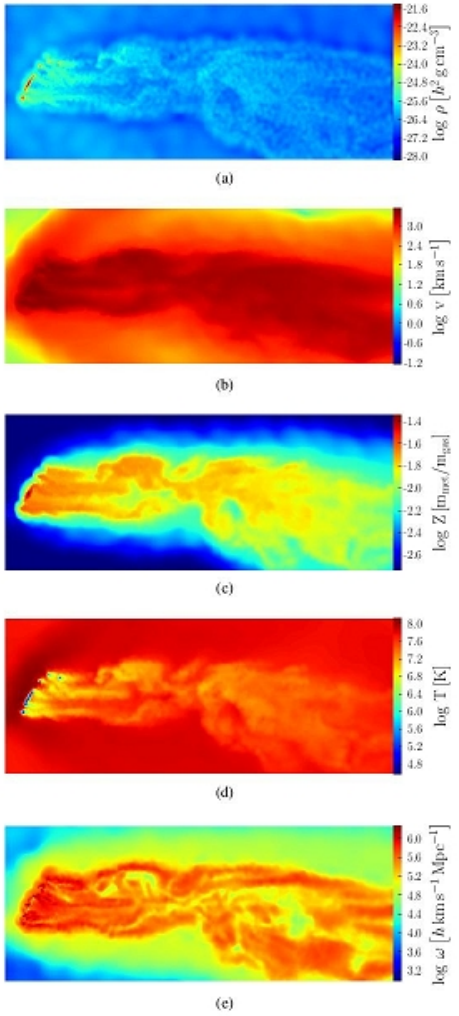

ıess $0.2\,h^{-1}$kpc and extension $100\,h^{-1}$kpc×$40\,h^{-1}$kpc through the galaxy and its wake in run S1.

Сравниваем влетевшую-полетавшую и изолированную

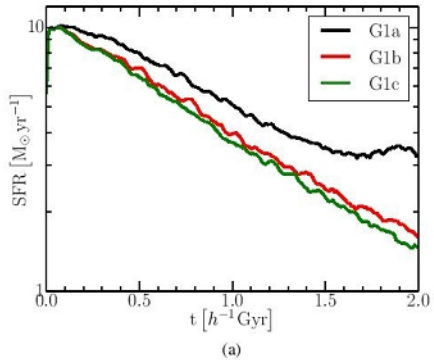

Fig. 4. (a) Star formation rate of model galaxy G1 when evolved in isolation. The three variants shown correspond to different gas masses in the corona. Model G1a has the same baryonic mass in the halo

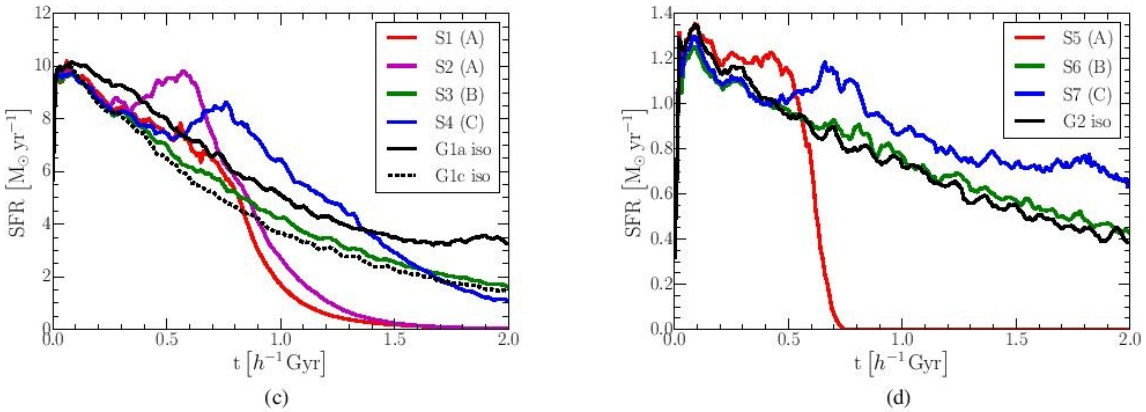

Fig. 9. (a,b) Evolution of the sSFR ≡ SFR h $M_\star^{-1}$ of model galaxies G1a, G1c, and G2 in isolation and cluster environments. The value of the main sequence of SF for the particular galaxy (black solid line) and 0.3 dex scatter (dashed black lines), taken from Schawinski et al. (2014), are shown. The grey shaded area indicates the region where they find 'green-valley' galaxies. (c,d) SFR of the model galaxies.

Вообще говоря, после ram pressure спирали никуда не исчезают…

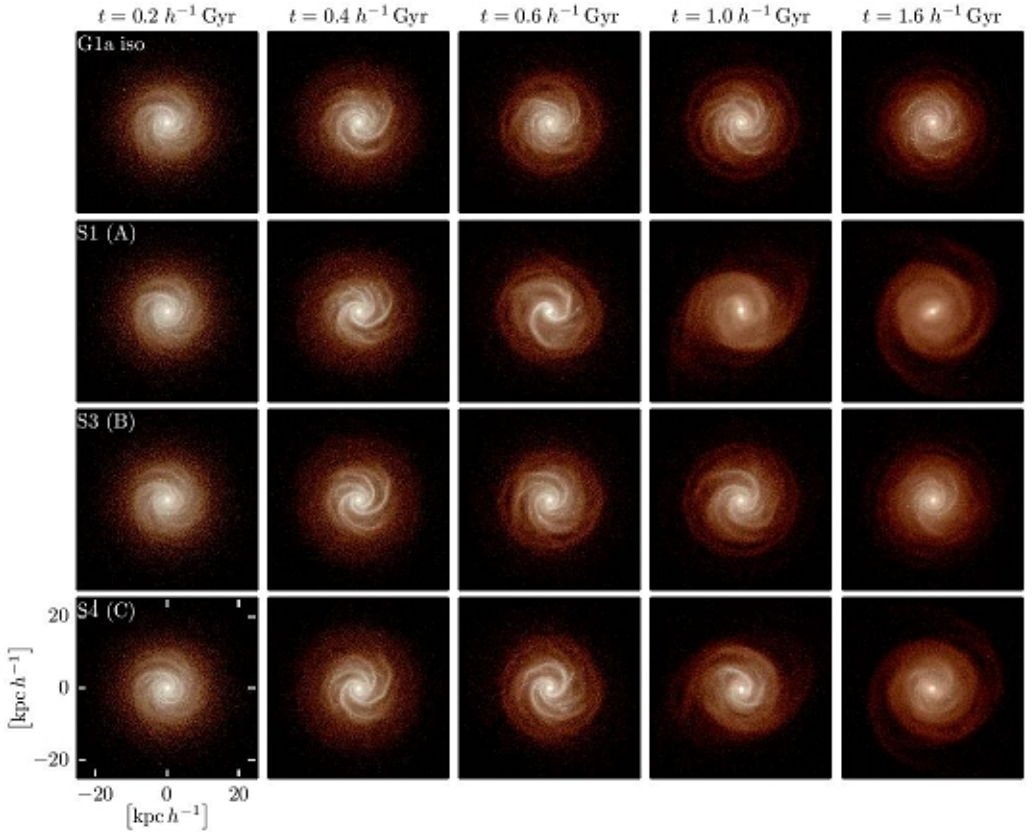

Fig. 12. Mock colour images of galaxy G1a in different environments. The evolution in isolation and runs S1, S3 and S4 are depicted in the different rows. In each column, the state at a selected time (indicated on top) is shown for each simulation.